Measurement of the $e^+e^- \to \pi^0\gamma$ cross section in the energy range 1.075–2 GeV at SND

M. N. Achasov,[1,2] A. Yu. Barnyakov,[1,2] K. I. Beloborodov,[1,2] A. V. Berdyugin,[1,2] D. E. Berkaev,[1,2] A. G. Bogdanchikov,[1] A. A. Botov,[1] T. V. Dimova,[1,2] V. P. Druzhinin,[1,2] V. B. Golubev,[1,2] L. V. Kardapoltsev,[1,2] A. S. Kasaev,[1] A. G. Kharlamov,[1,2] I. A. Koop,[1,2,3] A. A. Korol,[1,2] D. P. Kovrizhin,[1] S. V. Koshuba,[1] A. S. Kupich,[1,2] R. A. Litvinov,[1] K. A. Martin,[1] N. A. Melnikova,[1,2] N. Yu. Muchnoi,[1,2] A. E. Obrazovsky,[1] E. V. Pakhtusova,[1] K. V. Pugachev,[1,2] Yu. A. Rogovsky,[1,2] A. I. Senchenko,[1,2] S. I. Serednyakov,[1,2] Z. K. Silagadze,[1,2] P. Yu. Shatunov,[1,2] Yu. M. Shatunov,[1,2] D. A. Shtol,[1] D. B. Shwartz,[1,2] I. K. Surin,[1] Yu. V. Usov,[1] A. V. Vasiljev,[1,2] and V. V. Zhulanov[1,2]

[1]*Budker Institute of Nuclear Physics, SB RAS, Novosibirsk 630090, Russia*
[2]*Novosibirsk State University, Novosibirsk 630090, Russia*
[3]*Novosibirsk State Technical University, Novosibirsk 630092, Russia*

(Received 20 September 2018; published 5 December 2018)

The process $e^+e^- \to \pi^0\gamma$ is studied with the SND detector at the VEPP-2000 e^+e^- collider. Basing on data with an integrated luminosity of 41 pb^{-1} recorded in 2010-2012 we measure the $e^+e^- \to \pi^0\gamma$ cross section in the center-of-mass energy range from 1.075 up to 2 GeV. In the range 1.4–2.0 GeV the process $e^+e^- \to \pi^0\gamma$ is studied for the first time.

DOI: 10.1103/PhysRevD.98.112001

I. INTRODUCTION

In this paper we begin to study the $e^+e^- \to \pi^0\gamma$ process in experiments at the VEPP-2000 e^+e^--collider [1]. The previous most accurate measurements of this process were performed in experiments at the VEPP-2M e^+e^- collider with the SND [2–4] and CMD-2 [5] detectors.

The experimental data on the process $e^+e^- \to \gamma^* \to \pi^0\gamma$ is needed, in particular, for development of phenomenological models of the $\pi^0\gamma^{(*)}\gamma^{(*)}$ transition form factor used in the calculation of the hadronic light-by-light contribution to the value of the muon anomalous magnetic moment (see, e.g., [6]).

The energy dependence of the $e^+e^- \to \pi^0\gamma$ cross section is well described by the vector meson dominance (VMD) model. From the fit to the cross-section data the widths of radiative decays of vector mesons $\rho(770)$, $\omega(782)$, and $\phi(1020) \to \pi^0\gamma$ are extracted (see, e.g., [4]). These parameters are widely used in phenomenological models, in particular, to fix the vector-meson quark content [7]. It should be noted that currently the systematic uncertainties of some VMD-model parameters, such as the $\phi(1020) \to \pi^0\gamma$ width, and the relative phases between the $\rho(770)$, $\omega(782)$, and $\phi(1020)$ resonance amplitudes are determined by uncertainty in the contributions of excited vector states. The indications of the nonzero contribution of $\rho(1450)$ and $\omega(1420)$ resonances were obtained in Refs. [4,5], where the $e^+e^- \to \pi^0\gamma$ cross section was measured up to the center-of-mass energy $\sqrt{s} = 1.4$ GeV.

In this work, in the experiment with the SND detector at VEPP-2000, we repeat the measurement of the $e^+e^- \to \pi^0\gamma$ cross section in the energy range $\sqrt{s} = 1.075$–1.4 GeV and explore a new region, between 1.4 and 2 GeV.

II. EXPERIMENT

SND is a general-purpose non-magnetic detector. It was initially designed [8] for experiments at the VEPP-2M e^+e^- collider (1996–2000) and then was modified [9] for experiments at VEPP-2000, which began in 2010. The main part of SND is a spherical three-layer calorimeter containing 1640 NaI(Tl) crystals. The calorimeter covers a solid angle of 95% of 4π; its thickness for particles coming from the collider interaction region is $13.4X_0$. The calorimeter energy resolution for photons is $\sigma_E/E_\gamma = 4.2\%/\sqrt[4]{E_\gamma(\mathrm{GeV})}$, the angular resolution $\simeq 1.5°$. Directions of charged particles are measured by a nine-layer cylindrical drift chamber. Outside the calorimeter a muon detector is located, which consists of plastic scintillation counters and drift tubes. In this analysis the muon detector is used as a cosmic-ray veto.

The analysis presented in this paper is based on data with an integrated luminosity of 41 pb^{-1} recorded with the SND detector in 2010–2012 in the c.m. energy range $\sqrt{s} = 1.075$–2.000 GeV. The data were collected in

TABLE I. The c.m. energy ($E \equiv \sqrt{s}$), integrated luminosity (L), detection efficiency (ε), number of selected signal events ($N_{\rm sig}$), radiative-correction factor ($1+\delta$), measured Born cross section (σ). The radiative correction uncertainty is given in parentheses. For the cross section the first error is statistical, the second is systematic.

E, GeV	L, nb^{-1}	ε, %	$N_{\rm sig}$	$1+\delta$	σ, pb
1075	569	29.7	21 ± 10	1.32(6)	$93 \pm 45 \pm 4$
1119 (1100–1150)	2043	27.6	28 ± 17	1.02(6)	$48 \pm 29 \pm 3$
1200 (1175–1225)	2398	28.8	38 ± 16	0.92(2)	$60 \pm 26 \pm 2$
1284 (1250–1300)	3154	29.4	43 ± 18	0.92(2)	$50 \pm 21 \pm 2$
1353 (1325–1375)	2666	28.4	16 ± 14	0.94(3)	$23 \pm 19 \pm 1$
1425 (1400–1450)	3290	27.4	-12 ± 14	1.00(5)	$-13 \pm 15 \pm 1$
1509 (1475–1550)	4762	26.3	-14 ± 15	1.10(8)	$-11 \pm 13 \pm 1$
1607 (1575–1650)	3593	22.5	11 ± 13	1.06(16)	$12 \pm 16 \pm 2$
1705 (1675–1750)	3895	20.3	-1 ± 12	0.88(14)	$-1 \pm 13 \pm 2$
1804 (1760–1850)	5432	16.7	4 ± 14	0.91(6)	$4 \pm 15 \pm 1$
1926 (1870–2000)	8955	14.1	-9 ± 14	0.92(3)	$-8 \pm 13 \pm 1$

56 energy points during several c.m. energy scans. Due to relatively small statistics of $e^+e^- \to \pi^0\gamma$ events in the energy region under study the energy points are merged into 11 energy intervals listed in Table I.

For simulation of signal events, we use an event generator, which takes into account radiative corrections to the initial particles calculated according to Ref. [10]. The angular distribution of additional photons radiated by the initial electron and positron is simulated according to Ref. [11]. The event generator for the process $e^+e^- \to \gamma\gamma(\gamma)$ used for normalization is based on Ref. [12]. The theoretical uncertainty of the $e^+e^- \to \gamma\gamma$ cross section calculation is estimated to be 1%. Interactions of the generated particles with the detector materials are simulated using GEANT4 software [13]. The simulation takes into account variations of experimental conditions during data taking, in particular, dead detector channels, and beam-generated background. Due to the beam background, some part of data events contains spurious tracks in the drift chamber and photons. To take this effect into account, simulation uses special background events recorded during data taking with a random trigger, which are superimposed on simulated events.

III. EVENT SELECTION

In this analysis, we simultaneously select three-photon events of the process under study $e^+e^- \to \pi^0\gamma \to 3\gamma$ and two-photon events of the process $e^+e^- \to \gamma\gamma$ used for normalization. Some selection criteria, such as absence of charged tracks and extra photon in an event, and the muon-system veto, are common for both processes. So, systematic uncertainties associated with these criteria cancel as a result of the normalization.

The preliminary selection criteria for two- and three-photon events are following:

(i) No charged tracks are reconstructed in the drift chamber. The number of hits in the drift chamber is less than four.

(ii) The total energy deposition in the calorimeter is larger than $0.65\sqrt{s}$.

(iii) The total event momentum calculated using energy deposition in the calorimeter crystals is less than $0.3\sqrt{s}$.

(iv) No signal in the muon system.

Two-photon events of the process $e^+e^- \to \gamma\gamma$ are selected with the following additional criteria. There are exactly two photons in an event. Their energies is required to be larger than with $0.3\sqrt{s}$. The azimuthal and polar angles of the photons satisfy the conditions $||\phi_1 - \phi_2| - 180°| < 15°$, $|\theta_1 + \theta_2 - 180°| < 25°$, and $(180° - |\theta_1 - \theta_2|)/2 > 45°$. The integrated luminosity measured for each energy interval is listed in Table I. The systematic uncertainty on the luminosity measurement is estimated to be 1.4% and includes the theoretical error of cross section calculation (1%) and uncertainty associated with a difference between data and simulation in photon angular and energy resolutions (1%). The latter uncertainty was carefully studied in Refs. [4,14].

The $e^+e^- \to \pi^0\gamma$ candidate event must have exactly three reconstructed photons. The energy of the less-energetic photon in an event $E_{\gamma,\rm min}$ is required to be greater than 100 MeV. For these events we perform a kinematic fit with four constraints of energy and momentum balance. The condition on the χ^2 of the kinematic fit $\chi^2_{3\gamma} < 20$ is applied. For further selection we use the fitted parameters of the three photons. Their polar angles are required to be in the range $36° < \theta_\gamma < 144°$, and their energy be larger than $0.075\sqrt{s}$. The main source of background for the process under study is $e^+e^- \to 3\gamma$ events. They are strongly suppressed by the conditions on $E_{\gamma,min}$ and θ_γ. We calculate the mass recoiling against the most energetic photon in an event $M_{\rm rec}$ and select events with $80 < M_{\rm rec} < 190$ MeV$/c^2$.

The distribution of χ^2 of the kinematic fit ($\chi^2_{3\gamma}$) for data $e^+e^- \to \pi^0\gamma$ candidate events is shown in Fig. 1 as points with error bars. The histogram in Fig. 1 represents the

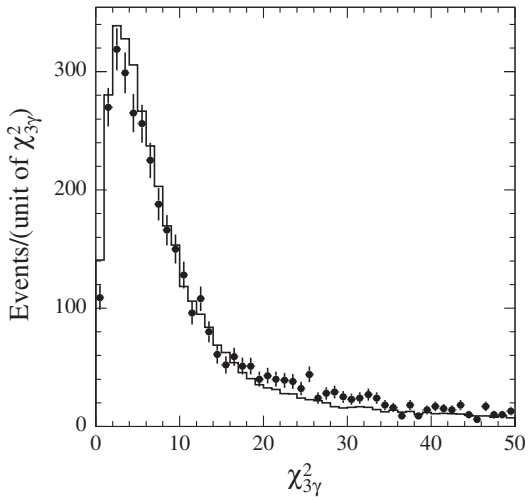

FIG. 1. The $\chi^2_{3\gamma}$ distribution for data (points with error bars) and simulated $e^+e^- \to 2\gamma(\gamma)$ events (histogram). The simulated distribution is normalized to the number of expected events.

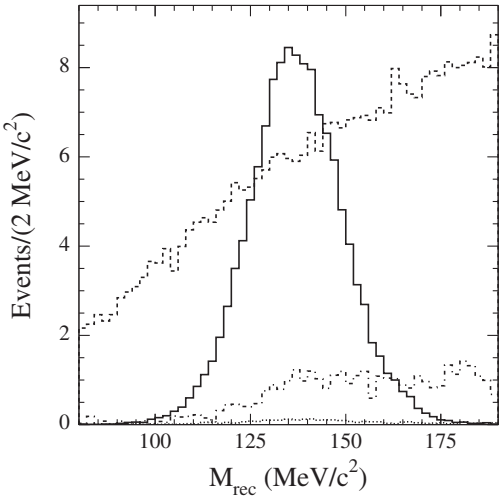

FIG. 2. The expected $M_{\rm rec}$ distributions (sum over all energy points) for signal (solid histogram) and ISR (dotted histogram), $e^+e^- \to 3\gamma$ (dashed histogram), and $e^+e^- \to \omega\pi^0$ (dash-dotted) backgrounds. The distribution for $e^+e^- \to 3\gamma$ events is multiplied by a factor of 0.1.

expected distribution for $e^+e^- \to 2\gamma(\gamma)$ events obtained using MC simulation. The number of events in the histogram is calculated as $\sum_i N^{\rm data}_{2\gamma,i}(N^{\rm MC}_{3\gamma,i}/N^{\rm MC}_{2\gamma,i})$, where $N^{\rm data}_{2\gamma,i}$ and $N^{\rm MC}_{2\gamma,i}$ are the numbers of selected $e^+e^- \to \gamma\gamma$ events in data and in $e^+e^- \to 2\gamma(\gamma)$ simulation, respectively, and $N^{\rm MC}_{3\gamma,i}$ is the number of three-photon events in the $e^+e^- \to 2\gamma(\gamma)$ simulation. It is seen that most of the selected data events originate from the background process $e^+e^- \to 3\gamma$. The difference between the tails of the data and MC distributions is due to the absence radiative corrections (extra photon radiation) to the $e^+e^- \to 3\gamma$ process in the $e^+e^- \to 2\gamma(\gamma)$ MC generator used.

IV. FITTING THE $M_{\rm rec}$ SPECTRA

The number of signal events ($N_{\rm sig}$) is determined from the fit to the $M_{\rm rec}$ spectrum by a sum of signal and background distributions. The signal distribution is described by a histogram obtained from $e^+e^- \to \pi^0\gamma$ simulation. The simulation includes radiation of an additional photon by the initial electron or positron. In particular, the initial-state radiation (ISR) process $e^+e^- \to \omega\gamma \to \pi^0\gamma\gamma$ is simulated. To correctly reproduce the rate of ISR events the event generator uses data on the Born $e^+e^- \to \pi^0\gamma$ cross section obtained in this work and Ref. [4] and fitted in the frame of the VMD model. The $M_{\rm rec}$ spectrum for simulated $e^+e^- \to \pi^0\gamma(\gamma)$ events is divided into two parts: with $2E_{\rm ISR}/\sqrt{s} < 0.4$ (signal) and $2E_{\rm ISR}/\sqrt{s} > 0.4$ (ISR background), where $E_{\rm ISR}$ is the energy of the extra photon emitted from the initial state.

The other sources of background for the process under study are $e^+e^- \to 3\gamma$ and $e^+e^- \to \omega\pi^0 \to \pi^0\pi^0\gamma$ events. The latter background is estimated using MC simulation and cross-section data obtained in Ref. [14]. Its fraction does not exceed 2% of the total background. The ISR background fraction is about 10^{-3}. The shapes of the signal and background distributions obtained using MC simulation are presented in Fig. 2. The simulation overestimates the number of background events by about 15%. In the fit to the $M_{\rm rec}$ spectrum, the background distribution is a sum of the ISR, 3γ, and $\omega\pi^0$ distributions plus a linear function. The latter is needed to take into account the difference between data and simulation in the shape of the background distribution and in the number of background events.

The results of the fit in the energy regions $\sqrt{s} =$ 1075–1375 MeV and $\sqrt{s} =$ 1400–2000 MeV are shown in Fig. 3. The fitted number of signal events in these two regions are 148 ± 34 and -26 ± 30. We do not observe an $e^+e^- \to \pi^0\gamma$ signal at $\sqrt{s} =$ 1400–2000 MeV. The obtained numbers of signal events for different energy intervals are listed in Table I.

V. DETECTION EFFICIENCY AND RADIATIVE CORRECTIONS

The visible cross section for the process $e^+e^- \to \pi^0\gamma$ is written as

$$\sigma_{\rm vis}(s) = \int_0^{x_{\rm max}} \varepsilon_r(s,x)F(x,s)\sigma(s(1-x))dx, \qquad (1)$$

where $\sigma(s)$ is the Born cross section extracted from the experiment, $F(x,E)$ is a so-called radiator function describing the probability to emit from the initial state extra photons with the total energy $x\sqrt{s}/2$ [10], $x_{\rm max} = 0.4$ (see Sec. IV), and $\varepsilon_r(s,x)$ is the detection efficiency. The detection efficiency is determined using MC simulation, as

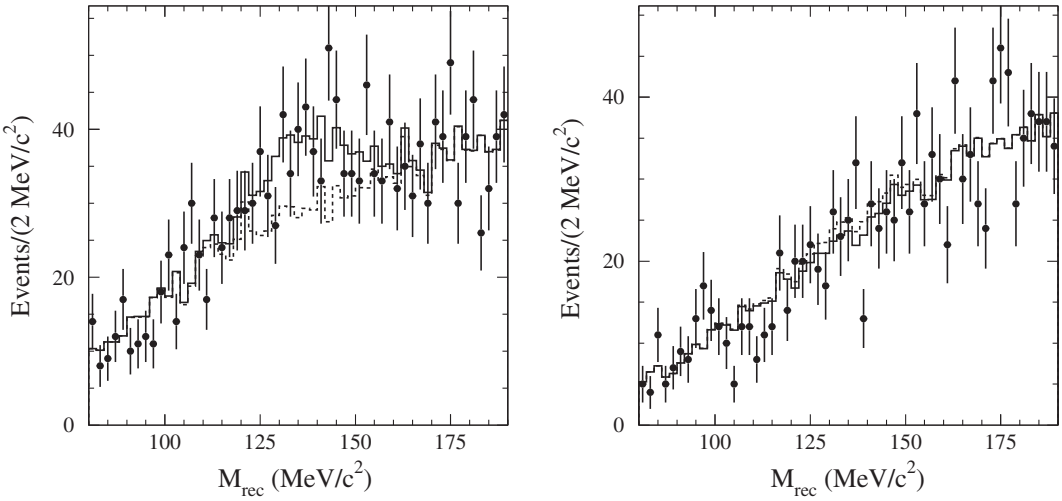

FIG. 3. The $M_{\rm rec}$ distribution for data events (points with error bars) with $\sqrt{s} = 1075$–1375 GeV (left), and $\sqrt{s} = 1400$–2000 MeV (right). The solid histogram represents the result of the fit described in the text. The dashed histogram shows the fitted background distribution.

a function of $\sqrt{s}$ and $x = 2E_{\rm ISR}/\sqrt{s}$. It is parametrized as $\varepsilon_r(s,x) = \varepsilon(s)g(s,x)$, where $\varepsilon(s) \equiv \varepsilon_r(s,0)$. We use the approximation when all variations of experimental conditions (dead calorimeter channels, beam background, etc.) are accounted for in $\varepsilon(s)$, while $g(s,x)$ is a smooth function of $\sqrt{s}$. With this parametrization, Eq. (1) can be rewritten in the conventional form:

$$\sigma_{\rm vis} = \varepsilon(s)\sigma(s)(1+\delta(s)), \tag{2}$$

where $\delta(s)$ is the radiative correction.

The functions $\varepsilon(s)$ and $g(s,x)$ are determined using MC simulation. Dependence of the $g(s,x)$ shape on s is not strong. The x dependence of the detection efficiency is shown in Fig. 4. Two effects determine the shape of the function $g(x)$. About 24% of ISR photons are emitted into the angular range covered by the SND calorimeter and may be detected and reconstructed if their energy higher than the photon reconstruction threshold 20 MeV. The sharp decrease of the efficiency at $x = 0.02$–0.04 is due to requirement that the number of reconstructed photons in an events is exactly 3, which removes events with a reconstructed ISR photon. The further decrease of the efficiency is due to the requirement of energy and momentum balance in an event (condition $\chi^2_{3\gamma} < 20$).

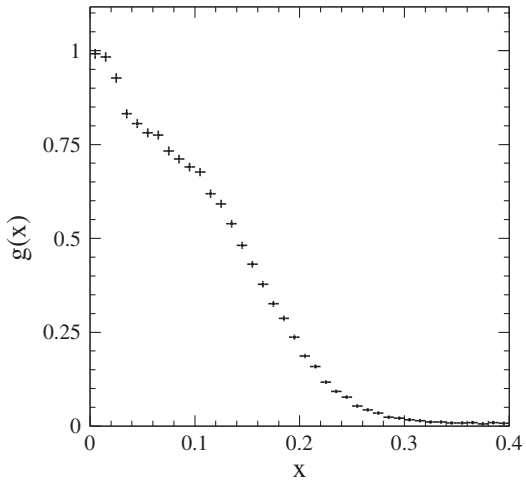

FIG. 4. The x dependence of the detection efficiency obtained from simulation for $\sqrt{s} = 1675$–2000 MeV.

The values of $\varepsilon(s)$ for different energy intervals are listed in Table I. It decreases with increasing $\sqrt{s}$ from 29% at 1075 MeV to 14% in the last energy interval $\sqrt{s} = 1870$–2000 MeV. The efficiency obtained using MC simulation is corrected (multiplied) by a factor of 1.013, which takes into account the difference between data and simulation in photon conversion in detector material before the tracking system (−0.3%) and in the shape of the $\chi^2_{3\gamma}$ distribution (1.6%). The conversion probability is measured using $e^+e^- \to \gamma\gamma$ events. To determine the efficiency correction for the $\chi^2_{3\gamma}$ cut and estimate systematic uncertainties due to imperfect simulation of the detector response for photons, we study simulated signal events and data events collected in 2013 in the maximum of the ω resonance, where the signal-to-background ratio is about 25. In particular, we loosen the condition $\chi^2_{3\gamma} < 20$ and vary the boundaries of the condition $36° < \theta_\gamma < 144°$. The systematic uncertainty in the detection efficiency is estimated to be less than 2%.

VI. FIT TO CROSS SECTION DATA

To determine radiative corrections and calculate the Born cross section, the energy dependence of the measured visible cross section $\sigma_{{\rm vis},i} = N_{{\rm sig},i}/L_i$ is fitted with Eq. (1).

The Born cross section is parametrized in the framework of the VMD model as follows (see, e.g., Ref. [15])

$$\sigma(s) = \frac{q_\gamma(s)^3}{s^{3/2}} \left| \sum\nolimits_V A_V(s) \right|^2, \tag{3}$$

$$A_V(s) = \frac{m_V \Gamma_V e^{i\varphi_V}}{m_V^2 - s - i\sqrt{s}\Gamma_V(s)} \sqrt{\frac{m_V^3}{q_\gamma(m_V^2)^3}\sigma_V}, \tag{4}$$

$$q_\gamma(s) = \frac{\sqrt{s}}{2}\left(1 - \frac{m_{\pi^0}^2}{s}\right), \tag{5}$$

where m_V is the V resonance mass, $\Gamma_V(s)$ is its energy-dependent width, $\Gamma_V \equiv \Gamma_V(m_V^2)$, φ_V is the interference phase, σ_V is the cross section at the resonance peak, which is related to the product of the branching fractions for the decays $V \to e^+e^-$ and $V \to \pi^0\gamma$:

$$\sigma_V = \frac{12\pi}{m_V^2} B(V \to e^+e^-) B(V \to \pi^0\gamma). \tag{6}$$

The sum in Eq. (3) goes over the resonances of the ρ and ω families, and $\phi(1020)$. To fix contributions of the $\rho(770)$, $\omega(782)$, and $\phi(1020)$ resonances, data obtained in this work are fitted simultaneously with the currently most precise $e^+e^- \to \pi^0\gamma$ data from Ref. [4] obtained at $\sqrt{s} < 1.4$ GeV.

The detailed description of fit parameters is given in Ref. [4]. The contribution of the excited vector states $\omega(1420)$, $\rho(1450)$, $\omega(1650)$, and $\rho(1700)$ are parametrized by a sum of two effective resonances (V' and V'') with masses of 1450 MeV and 1700 MeV. The V'' width is fixed at 315 MeV, the Particle Data Group (PDG) value for $\omega(1650)$ [16], while the V' width is a free fit parameter. The fitted value of $\sigma_{V''} = 2 \pm 10$ pb is consistent with zero. The fitted V' parameters are $\sigma_{V'} = 16 \pm 10$ pb, and $\Gamma_{V'} = 480 \pm 180$ MeV. The latter value is in agreement with the PDG values for $\omega(1420)$ and $\rho(1450)$ [16].

As result of the fit we calculate the radiative corrections and the experimental values of the Born cross section, which are listed in Table I. The radiative corrections are also calculated with the fitted V' parameters varied within their uncertainties, and $m_{V'}$ variation in the range 1450 ± 50 MeV. The maximum deviation of the radiative correction from its nominal value is taken as an estimate of its uncertainty. It is shown in parentheses in the $(1+\delta)$ column of Table I. It should be noted that the errors of the cross section measurement in Ref. [4] in the $\phi(1020)$ region and below give negligible contribution to the uncertainty of the radiative correction.

The quoted errors on the Born cross section are statistical and systematic. The latter includes the uncertainties in luminosity (1.4%), detection efficiency (2%), and radiative correction. The Born cross section measured in this work is shown in Fig. 5 in comparison with the previous measurements [4,5].

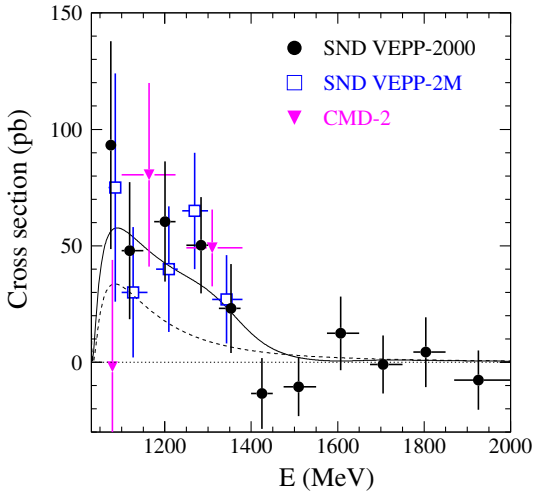

FIG. 5. The $e^+e^- \to \pi^0\gamma$ cross section measured in this work (SND@VEPP-2000) in comparison with the previous measurements: SND@VEPP-2M [4], and CMD-2 [5]. The solid curve is the result of the VMD fit with two excited resonances, V' and V''. The dashed curve represents the result of the fit with $\sigma_{V'} = \sigma_{V''} = 0$.

In the energy region below 1.4 GeV the obtained cross section is in agreement with the previous SND and CMD-2 measurements [4,5]. The curve shown in Fig. 5 is the result of the fit to SND data from the current analysis and Ref. [4]. The $e^+e^- \to \pi^0\gamma$ cross section in the energy region 1.4–2.0 GeV is consistent to zero. So, we do not observe the $\omega(1650)$ and $\rho(1700)$ decays to $\pi^0\gamma$ at the current level of statistics. To understand the significance of the contribution of the $\omega(1420)$ and $\rho(1450)$ states, we perform a fit with $\sigma_{V''} = 0$ and $\Gamma_{V'}$ fixed at the $\rho(1450)$ PDG value 400 MeV [16]. The fitted value $\sigma_{V'} = 13.2 \pm 5.6$ pb. This parameter is strongly correlated with the $\phi(1020)$ parameters, σ_ϕ and φ_ϕ. Therefore, we calculate the significance from the difference of the χ^2 values for this fit and a fit with $\sigma_{V'} = 0$. The χ^2/ν of the first fit is 47.9/66, where ν is the number of degrees of freedom, while the second is 58.5/67. The difference 10.5/1 has a probability of 1.19×10^{-3}, corresponding to 3.2σ. Compared with the previous SND measurement at VEPP-2M [4], adding new data increases the significance of the V' contribution by 1.1σ. Inclusion in the fit of the three CMD-2 data points [5] shown in Fig. 5 increases the V' significance up to 4σ. The dashed curve in Fig. 5 represents the result of the fit with $\sigma_{V'} = 0$. It is seen that almost all data points in the energy range 1.05–1.40 GeV obtained in this and previous experiments lie well above this curve.

VII. SUMMARY

The cross section for the process $e^+e^- \to \pi^0\gamma$ has been measured in the energy range of 1.075–2 GeV with the

SND detector at the VEPP-2000 e^+e^- collider. Below 1.4 GeV the obtained cross section is about 50 pb in agreement with the previous SND and CMD-2 measurements [4,5]. To explain this cross section value, the contribution of the $\omega(1420)$ and $\rho(1450)$ resonances is required with a significance of 4σ. In the region 1.4–2.0 GeV the process $e^+e^- \to \pi^0\gamma$ has been studied for the first time. The cross section in this region has been found to be consistent with zero within the statistical errors of about 15 pb.

ACKNOWLEDGMENTS

Part of this work related to the photon reconstruction algorithm in the electromagnetic calorimeter is supported by the Russian Science Foundation (Project No. 14-50-00080).

[1] A. Romanov *et al.*, in *Proceedings of the 25th Particle Accelerator Conference, PAC-2013, Pasadena, CA, 2013* (IEEE, New York, 2013), p. 14.
[2] M. N. Achasov *et al.* (SND Collaboration), Eur. Phys. J. C **12**, 25 (2000).
[3] M. N. Achasov *et al.* (SND Collaboration), Phys. Lett. B **559**, 171 (2003).
[4] M. N. Achasov *et al.* (SND Collaboration), Phys. Rev. D **93**, 092001 (2016).
[5] R. R. Akhmetshin *et al.* (CMD-2 Collaboration), Phys. Lett. B **605**, 26 (2005).
[6] M. Hoferichter, B. L. Hoid, B. Kubis, S. Leupold, and S. P. Schneider, J. High Energy Phys. 10 (2018) 141.
[7] P. J. O'Donnell, Rev. Mod. Phys. **53**, 673 (1981).
[8] M. N. Achasov *et al.* (SND Collaboration), Nucl. Instrum. Methods Phys. Res., Sect. A **449**, 125 (2000).
[9] M. N. Achasov *et al.*, Nucl. Instrum. Methods Phys. Res., Sect. A **598**, 31 (2009); V. M. Aulchenko *et al.*, Nucl. Instrum. Methods Phys. Res., Sect. A **598**, 102 (2009); A. Yu. Barnyakov *et al.*, Nucl. Instrum. Methods Phys. Res., Sect. A **598**, 163 (2009); V. M. Aulchenko *et al.*, Nucl. Instrum. Methods Phys. Res., Sect. A **598**, 340 (2009).
[10] E. A. Kuraev and V. S. Fadin, Yad. Fiz. **41**, 733 (1985) [Sov. J. Nucl. Phys. **41**, 466 (1985)].
[11] G. Bonneau and F. Martin, Nucl. Phys. **B27**, 381 (1971).
[12] F. A. Berends and R. Kleiss, Nucl. Phys. **B186**, 22 (1981).
[13] Geant4 Physics Reference Manual, in http://cern.ch/geant4/support/userdocuments.shtml.
[14] M. N. Achasov *et al.* (SND Collaboration), Phys. Rev. D **94**, 112001 (2016).
[15] N. N. Achasov, M. S. Dubrovin, V. N. Ivanchenko, A. A. Kozhevnikov, and E. V. Pakhtusova, Int. J. Mod. Phys. A **07**, 3187 (1992).
[16] M. Tanabashi *et al.* (Particle Data Group), Phys. Rev. D **98**, 030001 (2018).